Datkhile *et al. Cancer Nanotechnology* (2024) 15:43
https://doi.org/10.1186/s12645-024-00283-1

Cancer Nanotechnology

RESEARCH Open Access

Biosynthesized silver nanoparticles of *Cissus woodrowii* inhibit proliferation of cancer cells through induction of apoptosis pathway

Kailas D. Datkhile[1,2*], Pratik P. Durgawale[1], Nilam J. Jagdale[1], Ashwini L. More[1] and Satish R. Patil[1]

*Correspondence:
hodgeneticslab@kimskarad.in;
hodgeneticslab@kvv.edu.in

[1] Department of Molecular Biology and Genetics, Krishna Vishwa Vidyapeeth "Deemed to be University", Taluka-Karad, Karad, Satara 415539, Maharashtra, India
[2] Krishna Institute of Allied Sciences, Krishna Vishwa Vidyapeeth "Deemed to be University", Taluka-Karad, 415539 Karad, Satara, Maharashtra, India

Abstract

The purpose of this study was biogenic synthesis of silver nanoparticles using aqueous leaf extract of *Cissus woodrowii* (CW-AgNPs) and exploration of their role in inhibition cell proliferation of breast cancer cells. Inhibitory effect of biogenic CW-AgNPs on cell proliferation of MCF-7 cells was determined by MTT assay. Apoptotic cell death was demonstrated by caspase-3 assay, DNA fragmentation assay, Annexin-V-FITC/PI staining assay and cell cycle arrest assay by flow cytometry. Expression of apoptosis-related genes including caspase-3, p53 and Bcl2 was studied by western blot analysis and semi-quantitative RT-PCR. Results of UV–Vis spectrum of colloidal solution of CW-AgNPs showed surface plasmon resonance peak at 430 nm. TEM and XRD results confirmed spherical shaped, 20–30 nm sized nanoparticles. Cell proliferation results showed inhibitory effects of CW-AgNPs on MCF-7 with IC_{50} (24 h) 8.48 µg/mL and (48 h) 7.11 µg/mL. The CW-AgNPs altered cell morphology of MCF-7 cells and induced apoptosis significantly which was evidenced through caspase-3 activation and nuclear DNA fragmentation. The results were supported by the observation of Annexin-V-FITC/PI staining and cell cycle arrest assays. The up-regulated expression of both p53 and caspase-3 genes and down-regulation of Bcl2 at both protein and mRNA level supported their role in induction of apoptosis in MCF-7 cells in response to CW-AgNPs. The findings obtained in current study supported the role of biogenic CW-AgNPs in inhibition of cell proliferation in breast cancer cells through induction of apoptosis.

Keywords: *Cissus woodrowii*, CW-AgNPs, MCF-7, Apoptosis, Cell proliferation

Graphical Abstract

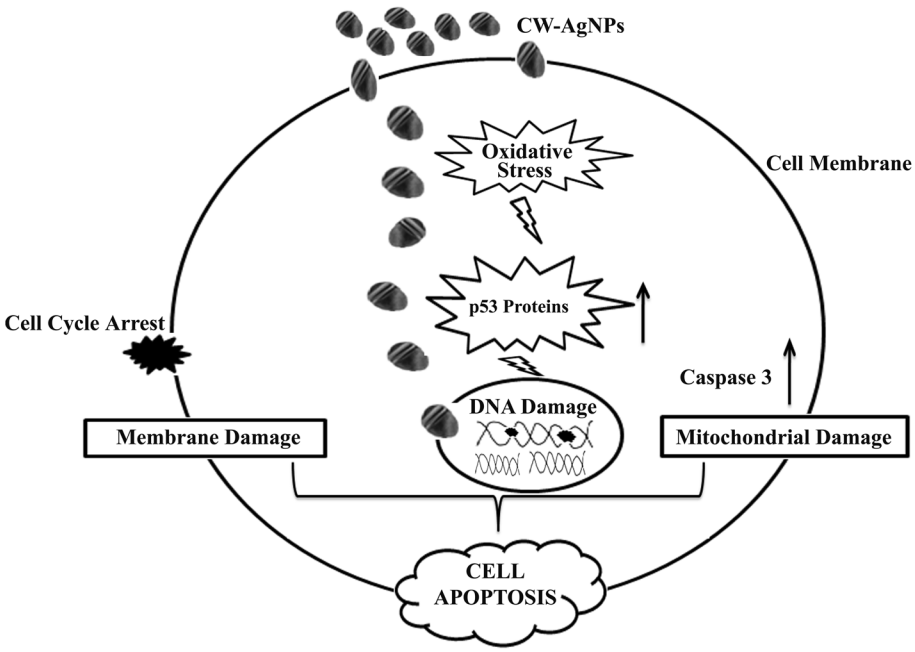

Possible mechanism of action of biogenic CW-AgNPs in MCF-7 cells

Introduction

Cissus woodrowii Cooke (Family: Vitaceae) commonly known as Woodrow's grape tree is a traditional medicinal plant endemic to Western Ghats of India. More than 20 different species of *Cissus* are widely studied for their pharmacological potential in terms of antioxidant, anti-inflammatory activities because of its main source of flavonoids, polyphenols, triterpenes, phytosterols, carotenoids and triterpenoids (Chi et al. 2010; Sawangjit et al. 2017; Kim et al. 2021). *Cissus quadrangularis* is one of the prominent species explored for its diverse bioactive compounds and their significant pharmacological properties (Gupta et al. 2018; Dhanasekaran 2020; Siddiqui et al. 2021). However, *Cissus woodrowii* is a lesser known species endemic to Maharashtra state of India, and remained largely unexplored for its phytochemicals and biomedical applications. This plant species have been understudied for its variety of phytoconstituents with significant biological activities. Preliminary studies have indicated that different parts of this plant possess metabolites containing flavonoids (rutin, quercitrin, hesperetin, and diosmetin) and polyphenols including catechins and epicatechins with significant bioactivities, such as anti-inflammatory, antioxidant, and antimicrobial properties (Kolap et al. 2020; Kolap et al. 2022; Patil et al. 2023, 2024). However, further research is warranted to validate these findings and explore the potential applications of *C. woodrowii* in developing new therapeutic agents.

Nanomedicine has emerged as a promising restorative tool in the twenty-first century for the effective management of various diseases, including cancer, lifestyle disorders as well as other infectious and non-infectious diseases. Nanomaterials have garnered

significant global attention due to their multifunctional importance in biomedical, pharmaceutical, and industrial applications (Langer and Weissleder 2015). These materials include inorganic metal nanoparticles (Yaqoob et al. 2020), magnetic nanoparticles (Ali et al. 2021), and the relatively new lipid and polymeric nanoparticles (Patra et al. 2018; Lu et al. 2021), all playing crucial roles in nanomedicine. Nanoparticles are functional nanomaterials emerged as potent therapeutic agents with their unique properties such as non-toxicity, natural antioxidant efficiency, biocompatibility, biodegradability and modulation of anticancer efficacy (Cordani and Somoza 2019; Yao et al. 2020). Silver and gold nanoparticles are commonly studied metal nanoparticles for their biogenic synthesis and numerous applications including anticancer potential (Naidu et al. 2015; Menon et al. 2017). Anticancer activities of biologically synthesized silver nanoparticles are studied against variety of cancers both in vitro and in vivo (Gomes et al. 2021; Jain et al. 2021; Al-Hhedhairy and Wahab 2022). Silver nanoparticles can act against cancer cells by modulating signaling pathways that lead to apoptotic cell death through oxidative DNA damage and ultimately cell shrinkage (Foldbjerg et al. 2011; Buttacavoli et al. 2018).

The process of biogenic synthesis of metal nanoparticles is based on redox reaction where the metal ions are reduced to stable nanoparticles by the active phytoconstituents present in plants (Gardea-Torresdey et al. 2003; Haverkamp and Marshall 2009). The hypothetical mechanism of silver nanoparticle synthesis is based on the fact that when metal salts are mixed with any plant extract, the silver ion interacts with water soluble compounds in plant extract through hydroxyl and carboxyl groups which help to transform the silver ions into silver nanoparticles (Huang et al. 2015, Singh et al. 2018). In last few years, green synthesis of metal nanoparticles using plant extracts have been extensively studied along with their biological potential (Yadi et al. 2018; Jadoun et al. 2022; Singh et al. 2023 Vijayaram et al. 2024). In addition, number of studies have reported synthesis of metallic nanoparticles using different species of *Cissus* and their diverse range of biological potentials including antioxidant (Rajeshkumar et al. 2019; Wu et al. 2020), antimicrobial (Marquis et al. 2016; Kalpana et al. 2017; Rajeshkumar et al. 2021; Kasi et al. 2021), anticancer potentials (Rajeshkumar et al. 2021; Sathappan et al. 2021). Biogenic synthesis of silver nanoparticles using *C. quadrangularis* has been documented along with their pharmacological applications (Renugadevi et al. 2012; Sudharameshwari and Maheshwari 2017; Gummapu and Amritkumar 2019; Kanimozhi et al. 2022; Ge et al. 2022). However, no other *Cissus* species have been studied for their appliance in green synthesis of silver nanoparticles except *C. rotundiflora* which have been reported as capping agent for synthesis of silver nanoparticles (Al-Ghamdi 2018).

The available literature information is insufficient to confirm the cytotoxicity prospective of biogenic silver nanoparticles synthesized using *C. woodrowii* (CW-AgNPs) against any of cancer cells with an intention to reveal their effects against cancer cell growth. In addition, the pattern of gene expression involved cell proliferation and apoptotic cell death in cancer cells in response to biogenic CW-AgNPs remained a scope of further research. Therefore, this study was aimed to synthesize silver nanoparticles (CW-AgNPs) using the aqueous leaf extract of *C. woodrowii* and evaluate their cytotoxic potential against the breast adenocarcinoma (MCF-7) cell line. We investigated the apoptosis pathway by examining the expression patterns of genes including p53, caspase-3, and Bcl2. Cell proliferation inhibition was assessed using the MTT assay, while

mRNA expression levels of the apoptosis-related genes were quantified by RT-PCR. Protein expression of apoptosis markers was analyzed by western blotting. In addition, the mechanism of apoptotic cell death was explored through caspase-3 assay and DNA fragmentation assay to detect oxidative DNA damage.

Materials and methods

Materials

Minimum essential medium (MEM), Fetal Bovine Serum (FBS), Trypsin–EDTA, and Penicillin–Streptomycin were purchased from Gibco. 3-(4,5-Dimethylthiazol-2-yl)-2,5-diphenyltetrazolium bromide (MTT) was obtained from Sigma, and Silver nitrate ($AgNO_3$), Triton X-100, phenylmethylsulphonyl fluoride (PMSF), Dithiothretol (DTT), Sodium dodecyl sulfate (SDS) were purchased from Sisco Research Laboratories. Caspase-3, p53, Bcl2 and anti-actin, goat anti-rabbit IgG and rabbit anti-mouse IgG antibodies were purchased from Abcam. WesternBright^{Tm} ECL detection system (Advansta), Verso cDNA synthesis kit, and Caspase-3 assay kit was purchased from Sigma-Aldrich. MCF-7 cell line used in this study was procured from National Centre for Cell Sciences, Pune, India.

Biosynthesis, purification and characterization of silver nanoparticles

Biosynthesis of silver nanoparticles was carried out by the reaction of 10 Milli-liter (mL) of aqueous extract of *C. woodrowii* with 90 mL of 1 milli-molar (mM) silver nitrate (AgNO3) solution. The mixture was incubated at 80 °C in dark with continuous agitation and monitored for the change in color of reaction mixture. During formation of biogenic CW-AgNPs, the reduction of silver nitrate by plant extract was monitored up to 3 h at 30 min interval. Preliminary characterization of biogenic silver nanoparticles was monitored by UV–Visible spectroscopy (UV–visible Dual Beam Spectrophotometer; UV-1800 Shimadzu) by scanning the spectrum of reaction mixture at 300 to 800 nm. The biosynthesized CW-AgNPs were characterized by Transmission Electron Microscopy (TEM) (Make: Jeol/JEM 2100), X-ray diffraction (XRD) (Make: (PXRD-6000 SCHIMADZU) and Fourier Transform Infrared Spectroscopy (FTIR) (Make: Thermo Nicolet Avatar 370 spectrometer) analysis at Sophisticated Analytical Instrument Facility at Sophisticated Test and Instrumentation Centre, Cochin University, Kerala.

In vitro evaluation of cell viability and cell proliferation

Cell line and cell culture

MCF-7 cell line used in this study was maintained in T-25 culture flasks containing MEM with 10% heat inactivated FBS and Penicillin (100 U/mL)–Streptomycin (100 µg/mL) under the conditions of 5% CO_2, 95% humidity and 37 °C temperature.

Cell viability/cell proliferation assay (MTT assay)

The inhibitory effect of biogenic CW-AgNPs on cell proliferation of MCF-7 cells was determined in vitro by MTT assay. In brief, 1×10^4 cells/well were seeded in 96-well plate in complete MEM medium with 10% FBS and allowed to grow at 5% CO_2, 95% humidity and 37 °C for 24 h (h) for recovery. The cells were then treated with different concentrations (2.5, 5, 7.5, 10, 12.5, and 15 µg/mL) of CW-AgNPs and incubated further

for 48 h at 37 °C and 5% CO_2, thereafter, 10 µl of 5 mg/ml concentration MTT was added to each well and further incubated at 37 °C, and 5% CO_2 atmosphere. After 4 h incubation, 200 µL of DMSO was added in each well to dissolve the formazan crystals. The absorbance of purple color developed was measured at 560 nm wavelength using UV–Vis 1800 spectrophotometer (Shimadzu) to determine percentage inhibition of growth of treated as well as untreated cells. The effect of the CW-AgNPs on the cell proliferation was expressed as the % growth inhibition, using the following formula: Percentage (%) inhibition = 100-(Abs560 nm of treated cells/Abs560 nm of control cells) × 100%.

Cell morphology

1×10^6 cells/well in 6-well plate containing MEM and 10% FBS were treated with 2.5, 5.0, 7.5, 10.0, 12.5 and 15.0 µg/mL concentrations of CW-AgNPs. After 24-h treatment with AgNPs, the change in cell morphology was observed under the phase contrast microscope (Primovert, Calr Zeiss).

Study of apoptosis

Caspase-3 assay

The activity of caspase-3 was measured in MCF-7 cells using caspase-3 assay kit (Sigma-Aldrich USA) according to the manufacturer's instructions. The control and CW-AgNPs (IC_{50})-treated cells were harvested after 24 h and washed with ice-cold PBS. Cells were lysed with 100 µL of lysis buffer (50 mM N-[2-Hydroxyethyl]piperazine-N′-[2-ethanesulfonic acid] (HEPES) (pH 7.4) and 5 mM 3-[(3-Cholamidopropyl) dimethylammonio]-1-propanesulfonate (CHAPS), 5 mM DTT) for 30 min at 4 °C. Protein extracts were collected after centrifugation at 12,000 ×g for 20 min. Equal volume (10 µl) of protein extracts were mixed with assay buffer (20 mM HEPES (pH 7.4), 0.1% CHAPS, 10 mM DTT, 1 mM ethylenediaminetetraacetic acid (EDTA)), and incubated with the caspase-3 substrate (acetyl-Asp–Glu–Val–Asp p-nitroanilide (Ac-DEVD-pNA) and caspase-3 inhibitor (Ac-DEVD-CHO) for 4 h and the absorbance was measured at 405 nm in a double-beam UV–Vis spectrophotometer. The assay was also performed with non-induced cells and in the presence of caspase-3 inhibitor for a comparative analysis.

DNA fragmentation assay

1×10^6 cells seeded in 6-well plates were treated with (IC_{50}: 8.48 µg/mL) of CW-AgNPs along with untreated controls and incubated at 37 °C in 5% CO2, for 24 h. The cells were lysed in 0.3 mL of cell lysis buffer containing 10 mM Tris–HCl, pH 7.5, 1 mM EDTA, 0.2% triton X-100, and 0.5% sodium dodecyl sulfate (SDS). The cell lysate was incubated with 0.5 mg/mL of RNase A at 37 °C for 1 h, thereafter, 0.2 mg/mL of proteinase K at 55 °C for 1 h. DNA in aqueous phase was precipitated by adding 1/10th volume of 5 M sodium chloride and equal volume of isopropanol at − 20 °C. After 1-h incubation, the suspension was centrifuged at 12,000 ×*g* for 30 min at 4 °C followed by DNA pellet wash by 70% ice-cold ethanol and air-dried DNA pellet was resuspended in $T_{10}E_1$ buffer (pH 8.0) and checked with 1.5% (w/v) low EEO agarose (Bangalore GeNei) gel containing 1 µg/mL ethidium bromide.

Annexin V-FITC assay

A total of 1×10^5 MCF-7 cells in 6-well plate were treated with CW-AgNPs (IC_{50}: 8.48 µg/mL) along with untreated control cells. After completion of 24-h incubation, cells were harvested and washed with ice-cold phosphate-buffered saline (PBS). Thereafter, apoptosis was detected by FITC-Annexin-V/Dead cell apoptosis kit (Invitrogen). The cells were resuspended in 1X annexin-binding buffer, thereafter stained with FITC-Annexin V at room temperature for 15 min. The stained cells were analyzed using Attune NxT flow cytometer at 488 nm dual wavelength with the Ex/Em (499/521). Detection of the green fluorescence of Annexin V-FITC was performed through the FITC channel (FL1 or BL1) detection.

Cell cycle arrest assay

1×10^5 MCF-7 cells were treated with CW-AgNPs (IC50: 8.48 µg/mL). After 24-h incubation, cells were harvested by trypsinization and washed with 1X PBS. Thereafter, 70% ethanol was added to cell pellet with brief vortex for the fixation of cells for 30 min at 4 °C. After incubation, cells were washed with 1X PBS to remove ethanol. After treatment with Rnase A, cells were stained with propidium iodide (100 µg/ml) as per the manufacturer's instructions for 30 min and the red fluorescence intensity was detected and recorded by Attune™ NxT Flow Cytometer, blue/red (Make: Thermo Fisher Scientific) in FL-2 or BL2 channels with the Ex/Em 499/521.

Western blot analysis of p53, caspase-3 and Bcl2

The total proteins of MCF-7 cells treated with CW-AgNPs (IC_{50}: 8.48 µg/mL) were isolated with protein homogenizing buffer containing 50 mM Tris, 5 mM EDTA, 0.1% Triton X-100, 1 mM PMSF, 0.5 mM DTT, and Protease Inhibitor cocktail. The resulting cell lysate was centrifuged at 15,000 rpm at 4 °C for 15 min and protein concentration was quantitated by Bradford protein assay kit (Bangalore GeNei). Equal amount of total protein (50 µg/lane) was resolved on 10% SDS-PAGE with 80 V for 2–3 h; thereafter, resolved proteins were then transferred on to nitrocellulose membranes. The membrane was blocked in Tris-buffer saline with Tween-20 (TBST) containing 5% casein with 1% BSA for 1 h followed by 1-h incubation with primary antibodies mouse anti-p53 (1:1000) and rabbit anti-caspase-3 (1: 5000), rabbit anti-Bcl2 (1:5000) and rabbit anti-actin (1:5000), and thereafter washing with TBST, the membranes were incubated with secondary antibodies (horseradish peroxidase-conjugated goat anti-rabbit IgG and rabbit anti-mouse IgG) (1:1000) for 1 h. The targeted protein bands were detected using Western Bright™ ECL enhanced Chemiluminescence kit (Advansta).

Reverse transcription-polymerase chain reaction (RT-PCR)

Total RNA was extracted from control and CW-AgNPs (IC_{50}: 8.48 µg/mL) treated MCF-7 cells using Trizol reagent. The cDNA was synthesized from equal amount of total RNA (5 µg) using Verso cDNA synthesis kit (Make: Thermo Scientific). Thereafter, 2 µL of each cDNA was amplified in a 20 µL PCR reaction mixture containing one unit Taq DNA polymerase, 2 µL 10X PCR buffer, 0.5 µL of dNTP (200 µM each)

Table 1 Oligonucleotide sequences of apoptotic genes used for expression studies by RT-PCR in response to CW-AgNPs treatment

Sr. no	Gene	Oligonucleotide sequence	Tm (°C)	Amplicon size (bp)
1	P53	FP 5′-ACTAAGCGAGCACTGCCCAA-3′ RP 5′-ATGGCGGGAGGTAGACTGAC-3′	54 56	175
2	Caspase-3	FP 5′-GTG GCA TTG AGA CAG ACA GTG G-3′ RP 5′-GCCAAG AAT AAT AAC CAG GTG C-3′	57 54	110
3	Bcl2	FP 5′-TGTGGCCTTCTTTGAGTTCG-3′ RP 5′-TCACTTGTGGCCCAGATAGG-3′	52 54	150
4	Actin	FP 5′-TCT GGC ACC ACA CCT TCT ACA ATG-3′ RP 5′-AGC ACA GCC TGG ATA GCA ACG-3′	57 56	200

and 10 pmol of respective primers as listed in Table 1. Cycling conditions comprised of an initial denaturation of 5 min at 94 °C followed by 30 cycles of amplification at (94 °C for 30 s, 55 °C for 30 s and 72 °C for 30 s) and final elongation step at 72 °C for 10 min. To control the PCR reaction components and the integrity of RNA, 2 µL of each cDNA sample was amplified separately for b-actin specific primers. Electrophoretic separation of amplification products was performed with 2.5% agarose gel in TBE buffer. Relative density of ethidium bromide-stained amplicons was determined using image analysis software Image Lab 3.0 software (BioRad, USA).

Statistical analysis

Statistical analyses were carried out for all assays performed in triplicate and the results were interpreted as mean ± SEM of three independent experiments. The IC_{50} values with 95% confidence interval are reported as mean ± SEM of three independent experiments. Significance of the difference between means of expression of genes from controls and CW-AgNPs tested samples was assayed using Student's *t* test. *p* value $^{***}p < 0.005$ was considered as level of significance. All statistical analyses were conducted using SPSS (IBM Version 20.0) software.

Results and discussion

Biosynthesis and characterization of CW-AgNPs

The phytosynthesis of nanoparticles is an emerging field in nanoscience research aiming to develop therapeutic treatments for cancer and other medical applications. A variety of secondary metabolites such as alkaloids, flavonoids, and polyphenols are important plant constituents considered for their pharmacological applications. Tremendous efforts have been made previously on the biosynthesis of silver and other metallic nanoparticles using various plants and their active constituents (Khandel et al. 2018; Datkhile et al. 2021; Chandralekha et al. 2021; Ari and Uddin 2021). However, there remained further scope to explore biosynthesis of metallic nanoparticles using many other shaded plant species. Keeping this in mind, we put an effort to synthesize silver nanoparticles using aqueous leaf extract of *C. woodrowii* and to assess their effects on cell proliferation and to explore underlying mechanism behind cell proliferation inhibition. Biogenic synthesis of silver nanoparticles using Woodrow's grape tree leaf extract was characterized by transformation of colorless solution of

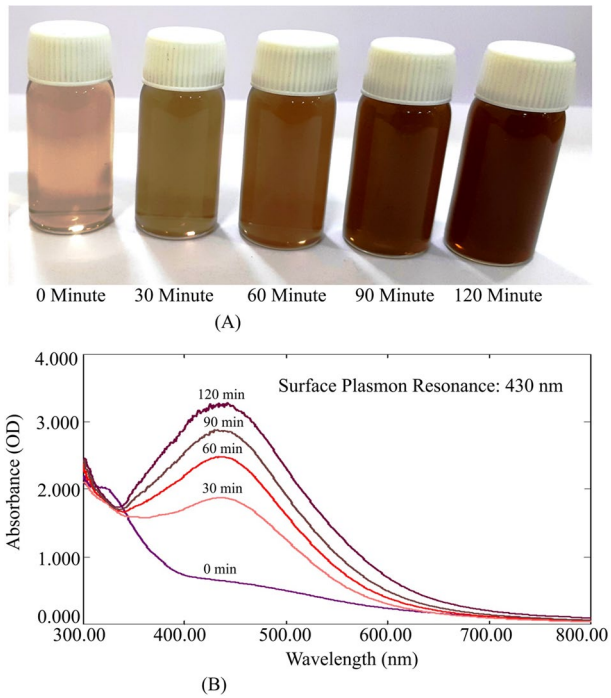

Fig. 1 Biosynthesis and characterization of silver nanoparticles using *C. woodrowii* leaf extract. **A** Time-dependent color change of colloidal solution of silver nitrate and aqueous extract of *C. woodrowii*. **B** The absorption spectrum of colloidal solution of AgNO3 and aqueous extract of *C. woodrowii* at different time intervals during the formation of CW-AgNPs

silver nitrate to brownish red color when incubated at 80 °C in dark with continuous agitation. This change in color of the reaction containing silver nitrate and aqueous extract validated conversion of metallic silver into silver nanoparticles (Fig. 1A). It was supported by the evidences from the literature that the active secondary metabolites including phenols, alkanes, ketones, alcohols, alkaloids, terpenoids and flavonoids present in plants can act as capping agents and help in bioreduction of silver ions into nanosilver during the formation of silver nanoparticles (Elavazhagan and Arunachalam 2011, Ahmad and Sharma 2012, Patra et al. 2015, Khan et al. 2016). Further, biosynthesized CW-AgNPs are characterized by UV–visible spectroscopy by measuring absorption spectra at 300–800 nm wavelengths. The bioreduction of silver ions to silver nanoparticles was monitored in a time-dependent manner by measuring the spectrum of colloidal solution at regular intervals of 30 min. The peak of surface plasmon resonance at 430 nm indicated synthesis of silver nanoparticles with different size range (Fig. 1B).

It was evident from the obtained results that bioreduction of AgNO3 in solution was started after 30 min of incubation and completed the process of AgNP synthesis after 120 min. Furthermore, morphology, size and shape of biosynthesized CW-AgNPs was demonstrated by TEM, which confirmed spherical shaped, 20–30 nm size range of CW-AgNPs (Fig. 2a–d).

The structural analysis of biogenic CW-AgNPs by XRD pattern showed characteristic peaks at 2θ values of 38.270°, 46.362°, 64.614° and 77.548° corresponding to 111,

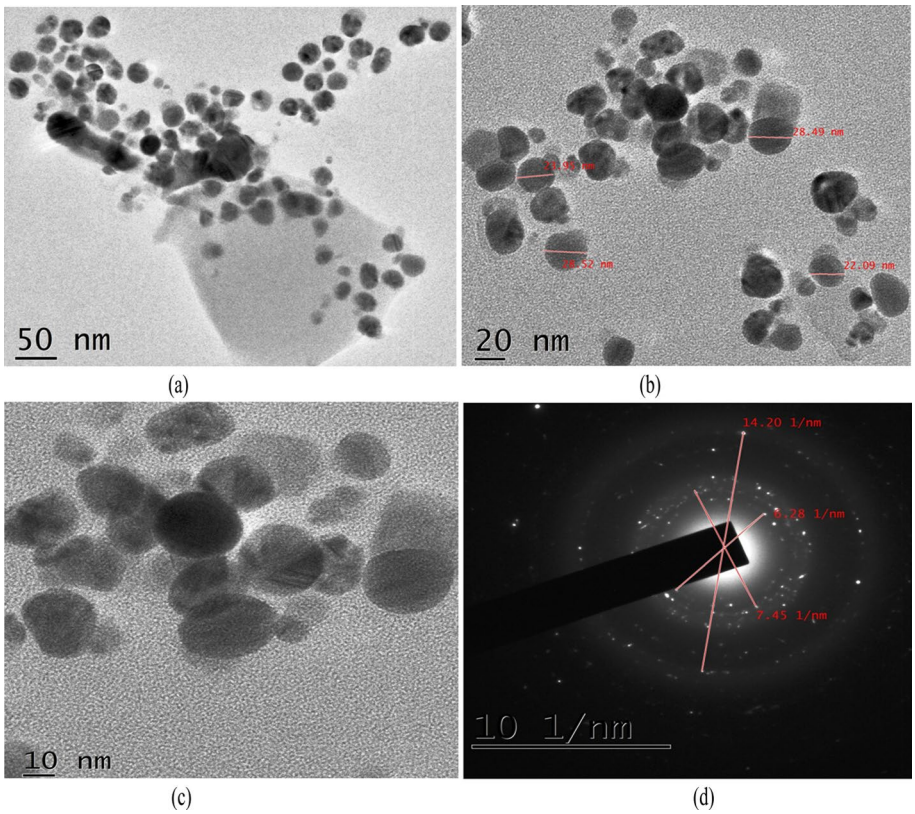

Fig. 2 Characterization of CW-AgNP nanoparticles: **a** TEM micrograph of CW-AgNPs, scale bar represents 50 nm. **b** High resolution of nanoparticles at 20 nm. **c** High resolution of nanoparticles at 10 nm. **d** SAED pattern

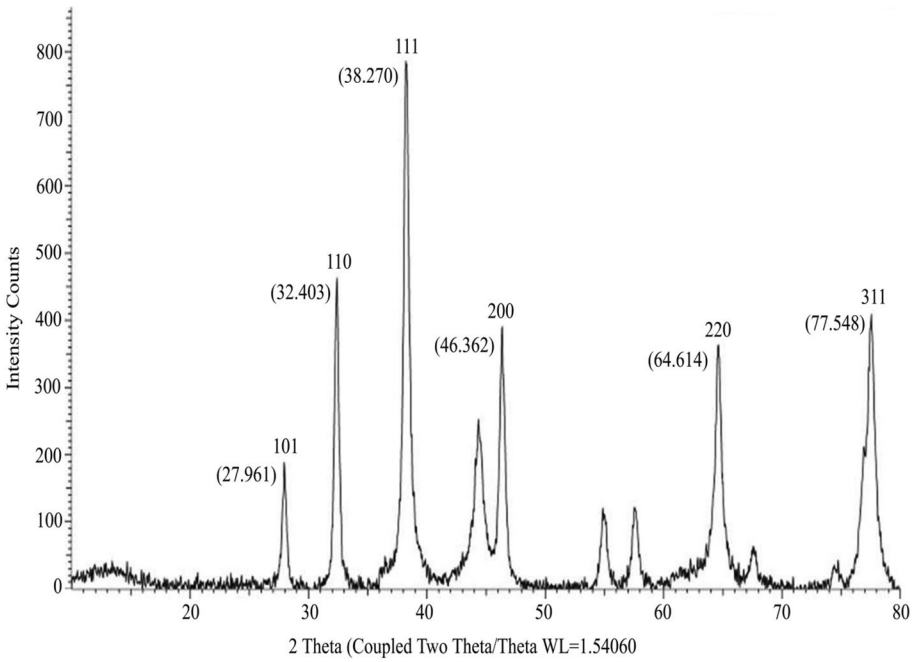

Fig. 3 XRD pattern of CW-AgNPs

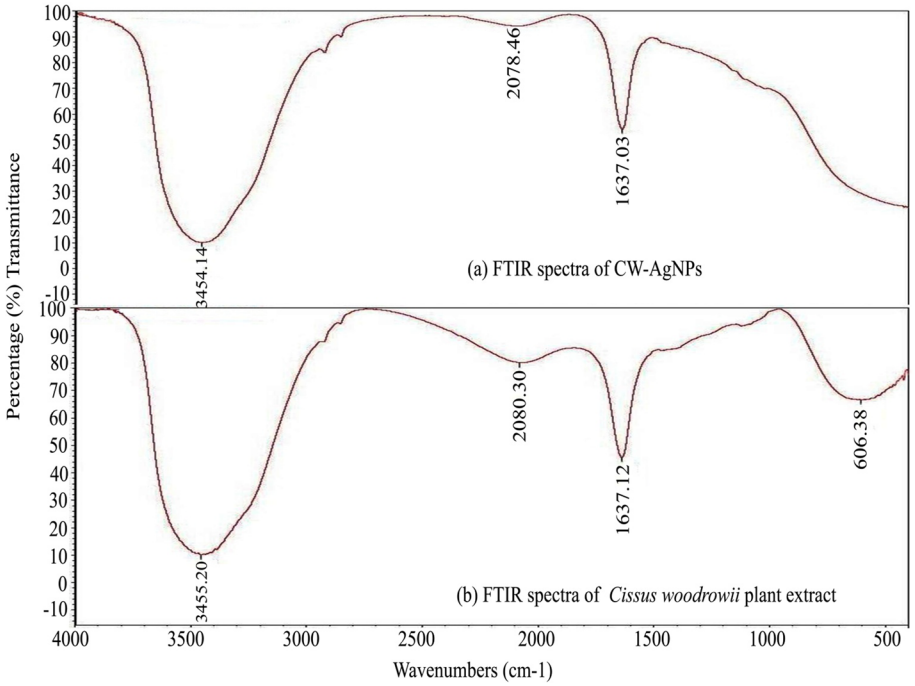

Fig. 4 FTIR spectra of **a** CW-AgNPs and **b** aqueous extract of *Cissus woodrowii*

200, 220, and 311 lattice planes of silver confirmed the crystalline nature of biogenic CW-AgNPs (Fig. 3).

Likewise, the confirmation of biogenic synthesis of silver nanoparticles using *C. woodrowii* was done by FTIR analysis which showed contribution of chemical functional groups (O–H, C = C) of phytocohemicals in the reduction and stabilization of CW-AgNPs. The FTIR spectra of both *C. woodrowii* and CW-AgNPs were recorded in the range of 500–4000 cm^{-1} for identification of functional groups accountable for bioreduction of silver ions into silver nanoparticles. The aqueous extract of *C. woodrowii* showed two major peaks at 3455.20 cm^{-1} and 1637.12 cm^{-1}; likewise, the CW-AgNPs showed peaks at 3454.14 cm^{-1} and 1637.03 cm^{-1}. The distinct peaks at 3455.20 cm^{-1} and 3454.14 cm^{-1} presented stretching vibration of O–H group of alcohol/phenol and 1637.12 cm^{-1} and 1637.03 cm^{-1} corresponded to stretching vibrations of C = C groups of amides/alkynes during the formation of CW-AgNPs (Fig. 4). The results of FTIR indicated the presence of O–H, C = C and CH groups which confirmed the presence of hydroxyl and carboxyl groups of flavonoids of plant extract. This indicated the role of phytoconstituents present in *C. woodrowii* in bioreduction of metallic sliver to silver nanoparticles (Ranoszek-Soliwoda et al. 2019).

Similarly, thermal stability in relation to weight of the biogenic CW-AgNPs was assessed using thermogravimetry. It was also noted from the results of TGA curve, that the weight loss of biogenic CW-AgNPs occurs in the temperatures between 290 °C and 395 °C (Fig. 5A). Further size distribution profile of CW-AgNPs was verified dynamic light scattering (DLS) analysis and noted smaller (15–20 nm) and medium (30–50 nm) sized nanoparticles (Fig. 5B).

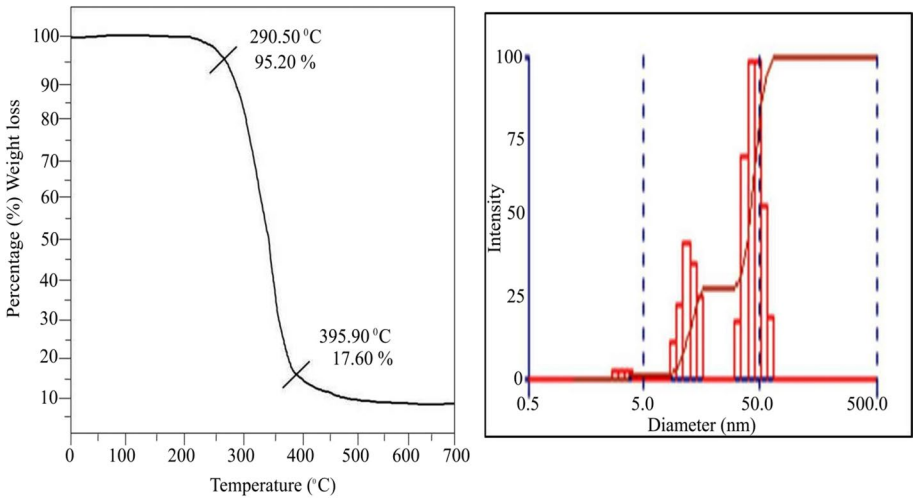

Fig. 5 **a** TGA thermograph of CW-AgNPs. **b** Particle size distribution of CW-AgNPs by DLS analysis

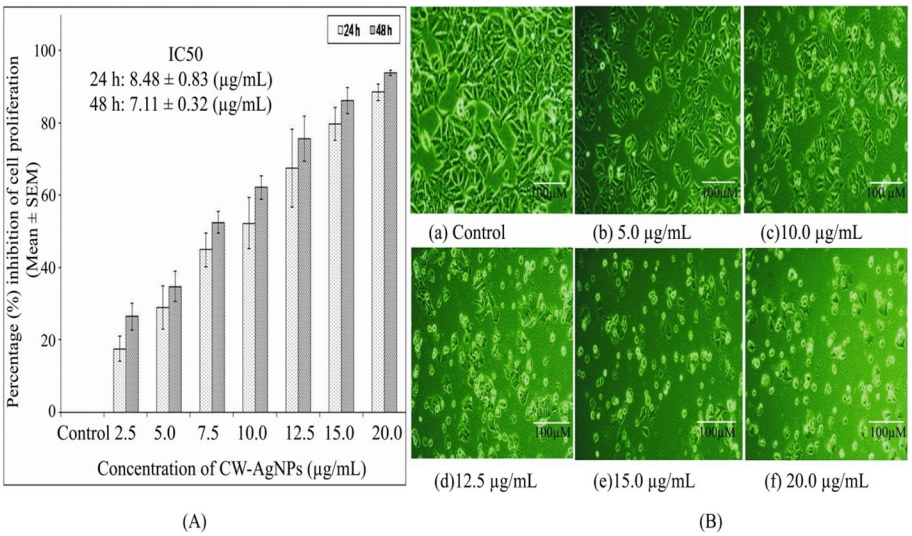

Fig. 6 Representative histogram showing dose-dependent cytotoxicity of biogenic CW-AgNPs on MCF-7 cells in vitro. **A** Inhibition of cell proliferation at different concentrations (2.5, 5, 7.5,10, 12.5,15 and 20 µg/ml) of CW-AgNPs was measured by MTT assay. The results represent the means of three independent experiments, and error bars represent the standard error of the mean. **B** Cell morphology of MCF-7 cells after 24-h treatment of biogenic CW-AgNPs, at different concentrations **b** 5, **c** 10, **d** 12.5, **e** 15 and **f** 20 µg/ml. All images are taken at 20× magnification with Carl Zeiss phase contrast microscope; scale bars, 100 µm

Biogenic CW-AgNPs inhibit cell proliferation in breast cancer MCF-7 cells

The biosynthesized CW-AgNPs were studied in vitro for their inhibitory effects against cell proliferation of breast cancer (MCF-7) cells. Cytotoxicity results for the effects of CW-AgNPs exerted significant inhibition of cell proliferation in the studied cancer cells in dose and time-dependent manner (2.5–20.0 µg/mL) (Fig. 6A). It was significant from the obtained MTT assay results that when MCF-7 cells were treated to higher concentration of CW-AgNPs, it lead to 88.61 ± 2.35% and 93.97 ± 0.78% of cell proliferation inhibition, after 24-h and 48-h exposure, respectively. The biosynthesized CW-AgNPs

exhibited effectual cytotoxicity towards cancer cell lines where 50% inhibitory concentrations (IC50) of (MCF-7: 8.48 µg/mL; 7.11 µg/mL) were recorded, respectively, after 24 and 48 h of exposure. The maximum inhibition of growth of MCF-7 cells occurred when exposed to 20 µg/mL concentrations of CW-AgNPs which were similar to the cytotoxicity effects of aqueous and ethanolic extract of *C. woodrowii* leaves. The morphological alterations such as shrunken appearance wee observed in cancer cells when exposed to 5.0 µg/mL and higher concentrations of CW-AgNPs (Fig. 6B), whereas untreated control looks intact with healthy appearance.

It was evident from earlier reports that biogenic nanoparticles can effectively induce intracellular suicide in cancer cells by altering the cell membrane integrity which lead to cell shrinkage, condensation of cytoplasm, cell growth arrest and ultimately apoptotic cell death. Earlier reports communicated the biogenic nanoparticles from different plant source and their cytotoxicity potentials against variety of cancer cells where nanoparticles are studied in vitro using human breast cancer (Gurunathan et al. 2013), cervical adenocarcinoma (Datkhile et al. 2020), hepatocellular carcinoma (Al-Hhedhairy and Wahab. 2022), and lung cancer (Mejia-Mendez et al. 2023). Similarly, researchers established biosynthesis of metal nanoparticles such as copper nanoparticles using *C. arnotiana* (Rajeshkumar et al. 2019), *C. quadrangularis* (Rajeshkumar et al. 2021; Kasi et al. 2021), zinc oxide nanoparticles using *C. quadrangularis* (Kalpana et al. 2017; Sathappan et al. 2021) and calcium oxide nanoparticles using *C. quadrangularis* plant extract (Marquis et al. 2016). The biological potentials including antioxidant, antibacterial, and anti-inflammatory effects of such metallic nanoparticles were highlighted in earlier reports. In addition, documented evidences explicated synthesis of biogenic silver nanoparticles using *C. quadrangularis* and their pharmacological properties including antioxidant and antibacterial activities (Renugadevi et al. 2012; Kanimozhi et al. 2022; Ge e al. 2022). Earlier studies by Renugadevi et al. showed cytotoxicity activity of silver nanoparticles synthesized using *C. quadrangularis* against larynx epithelioma cell line (Hep-2) with IC50 of 64 µg/ml where minimum concentration of 20 µg/ml showed 12% cytotoxicity (Renugadevi et al. 2012). Gummapu and Amritkumar confirmed the cytotoxicity of CQ-AgNPs against HeLa and lung cancer A549 cell line, where 20 µg/ml of AgNPs caused 36% of inhibition of HeLa cells and 70% of inhibition occurred at 160 µg/ml concentration (Gummapu and Amritkumar 2019). Very recently, Ge et al. (2022) studied anticancer properties of CQ-AgNPs against colon cancer HT-29 cell line where 40–60% inhibition of cell proliferation occurred at the 100 µg/ml concentrations of AgNPs. Our results highlighted strong cytotoxic activity of CW-AgNPs against MCF-7 cells, demonstrating a much greater efficacy than previously reported. While researchers have assessed the cytotoxic potential of AgNPs synthesized using other *Cissus* species, none of these studies have detailed the mechanisms underlying the inhibition of cell proliferation and the induction of apoptotic cell death. This gap in research points to the need for further investigation into the specific pathways and molecular interactions involved. In this regard, we designed an experiment to discover the mechanism of action of CW-AgNPs on cell proliferation and to explore the status of apoptosis signatures in MCF-7 cells in response to biogenic CW-AgNPs. The biosynthesized CW-AgNPs exerted significant anti-proliferative action against breast adenocarcinoma cells with IC50 of 8.48 ± 0.83 µg/mL and 7.11 ± 0.32 µg/mL after 24 h and 48 h post-AgNPs

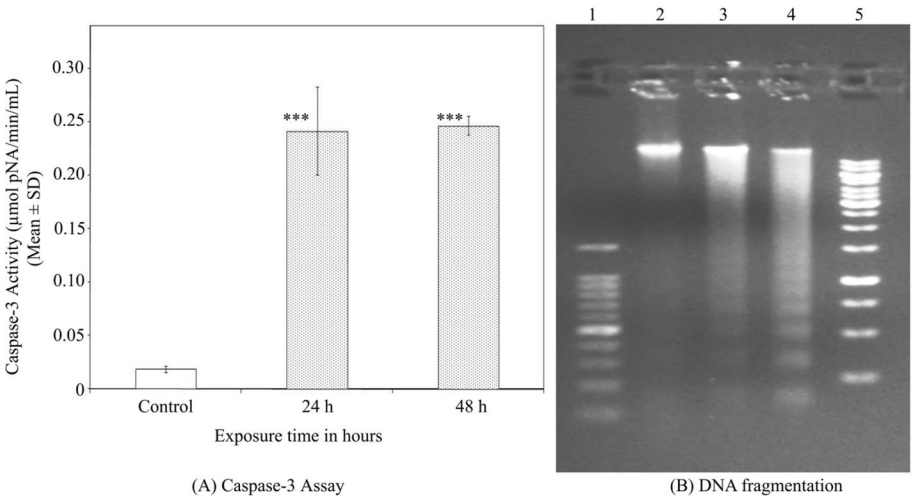

Fig. 7 **A** Representative histogram showing caspase-3 activity in (MCF-7 cells. Error bars indicate the standard error of the mean (SEM) for three independent experiments ($n = 3$). Levels of significance in caspase-3 activity, µmolpNA/min/ml between control and NFAgNPs exposed samples assessed by Student's *t* test are marked by (***$p < 0.005$), which found to be increased significantly in protein samples obtained from 24 and 48 h post-exposure periods. **B** Representative agarose gel images showing DNA fragmentation in MCF-7 cells treated with CW-AgNPs at 8.48 µg/ml concentration. Lane 1 is 100 bp DNA marker: Lane 2 is DNA from control cells followed by lane 3: 24 h and lane 4: 48 h, Lane 5 is 1 Kb DNA marker

exposure. The cell morphology was extensively altered with shrunken appearance and loss of membrane integrity which was evident in cells treated with 15 µg/mL and higher concentrations of CW-AgNPs.

Biogenic CW-AgNPs induced apoptosis in MCF-7 cells through cell cycle arrest, caspase-3 activation and DNA damage

Induction of apoptosis is an organized event which program the cells to die when received specific stimulus and controls the cell growth. To confirm above mentioned hypothesis, we assumed apoptotic effects of CW-AgNPs towards cancer cells which were demonstrated by caspase-3 activation and DNA fragmentation assay. The obtained results revealed caspase-3 activation as one of the attribute towards apoptosis in MCF-7 cells exposed to different concentrations CW-AgNPs for 24 h. The cancer cells showed significantly increased caspase-3 activity when treated with CW-AgNPs ($p < 0.005$) as compared to unexposed control cells as depicted in Fig. 7A. In addition to this, induction of apoptosis in selected cells was further confirmed by DNA fragmentation pattern. The cellular DNA fragmentation is considered as distinct hallmark of programmed cell death or apoptosis. When the cells were treated with CW-AgNPs, the apoptotic cells showed characteristic extensive double-strand breaks in cellular DNA thereby yielding ladder appearance (Fig. 7B, Lane 3–4), whereas DNA from untreated control cells did not exhibit prominent DNA fragmentation (Fig. 7B, Lane 2) when resolved by agarose gel electrophoresis. This extensive DNA double-strand breaks observed in treated cells evidenced induction of apoptosis.

The results of flow cytometry analysis with Annexin-V-FITC/PI dual staining confirmed apoptotic cell death in MCF-7 cells in response to CW-AgNPs. The MCF-7 cells treated with 8.48 µg/mL concentrations of CW-AgNPs for 24 h showed significant

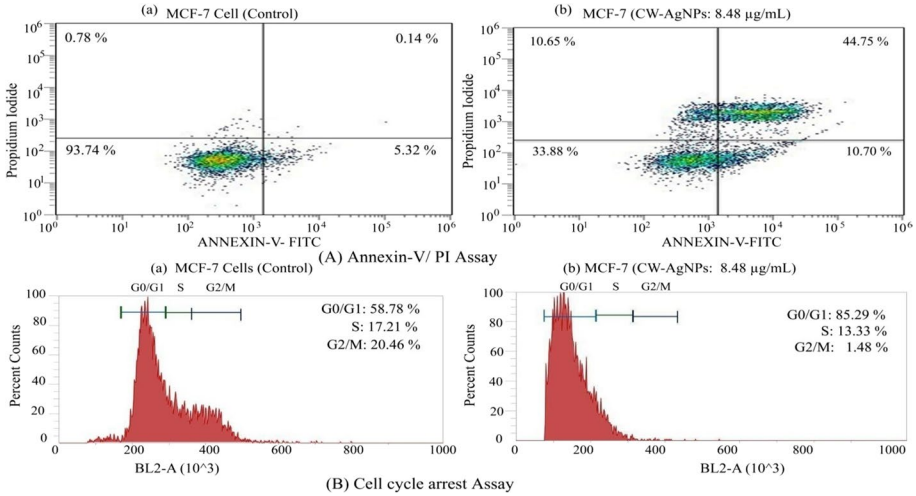

Fig. 8 **A** Confirmation of apoptosis by Annexin-V-FITC/PI staining assay. **a** Control MCF-7 cells. **b** MCF-7 cells treated with IC50: 8.48 µg/ml CW-AgNPs for 24 h. The cells were stained with Annexin-V-FITC and propidium iodide and the percentage of apoptotic cell population was analyzed by flow cytometry. **B** Cell cycle arrest assay where **a** control cells and **b** MCF-7 cells were treated with 8.48 µg/ml CW-AgNPs for 24 h and the cell cycle distribution was analyzed by flow cytometry

early (10.70%) and late (44.75%) apoptosis as compared to unexposed controls (Fig. 8A). These results demonstrated that biogenic CW-AgNPs induces cell death in breast adenocarcinoma cells by means of early and late apoptosis. The results of cell cycle analysis indicated apoptotic cell death of MCF-7 cells in response to CW-AgNPs was due to cell cycle arrest. The MCF-7 cells were treated with 8.48 µg/mL of CW-AgNPs for 24 h thereafter stained with PI and evaluated with flow cytometry. It was evident from the results that, the cell cycle was arrested at G2/M phase in MCF-7 cells exposed to CW-AgNPs (Fig. 8B).

Biogenic CW-AgNPs altered expression of p53, caspase-3 and Bcl2 genes in MCF-7 cells

The activation of tumor suppressor p53 protein and caspase-3 is known for their role in cell cycle arrest in response to stressors (Nagarajan et al. 2019; Kumari et al. 2020). In view of this, when MCF-7 cells were exposed to CW-AgNPs, significant up-regulated expression of both caspase-3 and p53 was noted, and Bcl2 was considerably down-regulated after 24 h of nanoparticle treatment which indicated the induction of cell apoptosis through activation of apoptotic genes. Western blot analysis was used to verify the fate of apoptosis pathway genes including p53, caspase-3 and Bcl2 at protein level from cancer cells exposed to biogenic CW-AgNPs. The expression of p53 and caspase-3 proteins showed significant increase in selected MCF-7 cells in response to exposure of biogenic CW-AgNPs. Significant differences were noted in protein level expression of both caspase-3 and p53 in CW-AgNPs exposed cells, as compared to their respective untreated controls ($p < 0.005$) (Fig. 9A, B). However, the Bcl2 protein decreased significantly post-CW-AgNPs exposure. The housekeeping actin was employed as loading control which indicated identical intensity bands which provides equivalent concentration in all samples. Similarly, expression pattern of apoptosis pathway genes at mRNA level was evident from the results of real

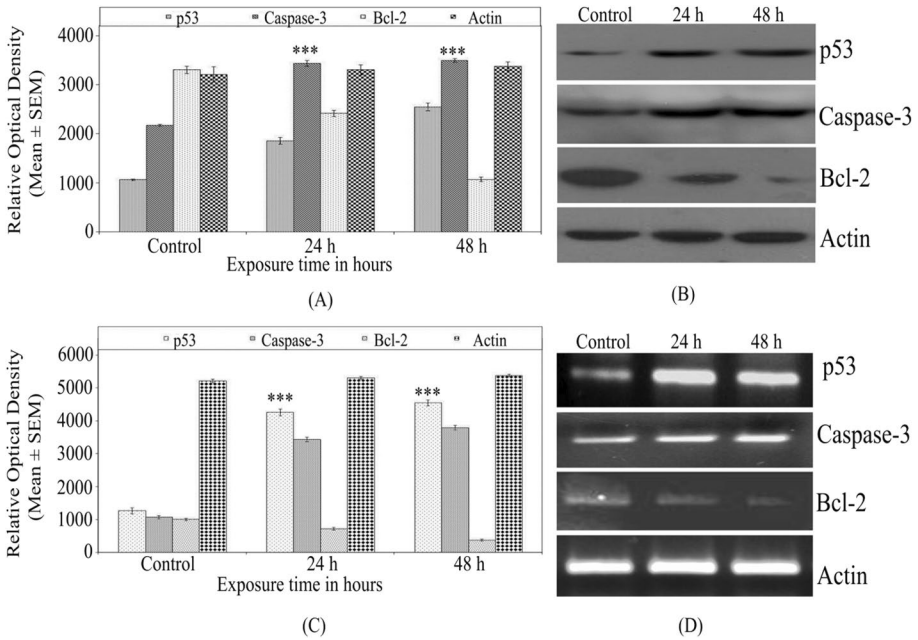

Fig. 9 **A** Representative histogram showing relative levels of p53, caspase-3, Bcl2 proteins from MCF-7 cells resolved in western blot were quantitated by densitometric analysis. Error bars indicate the standard error of the mean (SE) for three independent experiments ($n = 3$). Significant differences assessed by Student's t test are indicated by (***$p < 0.005$) and are found to be increased significantly in samples obtained from 24-h and 48-h post-exposure periods as compared to control. **B** Representative western blot showing expression of p53, caspase-3 and Bcl2 protein from MCF-7 cells exposed to IC_{50} concentration (8.48 µg/ml) of CW-AgNPs with different time points (24 h and 48 h) ($N = 3$). Lane 1 is control; lanes 2 and 3 are cell protein extracts from CW-AgNPs exposed samples at 24-h and 48-h exposure time. **C** Representative histogram showing relative levels of p53, caspase-3, and Bcl2 cDNA of MCF-7 cells. Significant differences in levels of p53 and caspase-3 are indicated by (***$p < 0.005$) and found to be increased significantly in samples obtained from 24-h and 48-h post-exposure periods as compared to control. **D** Representative amplicons of p53, caspase-3, Bcl2 and Actin genes from MCF-7, cells exposed to IC_{50} concentration (8.48 µg/ml) of CW-AgNPs. Lane 1 is control; lanes 2 and 3 are mRNA levels from CW-AgNPs exposed samples at 24-h and 48-h exposure time

time PCR. The results of semi-quantitative RT-PCR were expressed in fold change of mRNA expression levels, where statistically significant 3–fourfold change of both caspase-3 and p53 mRNA expression level were noted in CW-AgNPs treated cells (Fig. 9C, D). The mRNA expression levels of p53 and caspase-3 mRNA were up-regulated significantly in ($p < 0.005$) in MCF-7 cells by treatment of CW-AgNPs.

Conclusion

To the best of our knowledge, this is the first study of its kind to synthesize and characterize silver nanoparticles using aqueous extract of *C. woodrowii* leaves. We have reported fast process of biogenic silver nanoparticles synthesis with crystalline and spherical shaped, 15–30 nm sized CW-AgNPs. It was evident from the findings obtained from current study that biogenic CW-AgNPs inhibited cell proliferation in breast adenocarcinoma cells through activation of apoptosis inducing genes including p53 and caspase-3 which was confirmed through RT-PCR and western blotting. The cell cycle arrest was evident at G2/M phase in MCF-7 cells after 24 h of CW-AgNPs treatment.

Acknowledgements
The authors gratefully acknowledge all the facilities and financial support provided by the Krishna Vishwa Vidyapeeth (Deemed to be University), Karad, India for experimental work. The authors are thankful to Mr. Santosh Jadhav for technical support.

Author contributions
Concept: KDD, SRP; design: KDD; experimental studies: PPD, NJJ, ALM; data analysis: KDD, PPD; statistical analysis: KDD, PPD; manuscript preparation: KDD, PPD; all the authors read and approved the final manuscript.

Funding
Intramural funding by Krishna Vishwa Vidyapeeth (Deemed to be University).

Availability of data and materials
Not applicable.

Declarations

Ethics approval and consent to participate
Not applicable.

Consent for publication
Not applicable.

Competing interests
None of the author declares financial or any other competing interests.

Received: 19 June 2024 Accepted: 30 July 2024
Published online: 09 August 2024

References

Ahmad N, Sharma S (2012) Green synthesis of silver nanoparticles using extracts of *Ananas comosus*. Green Sustain Chem 2:141–147
Al-Ghamdi AY (2018) Antibacterial activity of green synthesis silver nanoparticles using some wild edible plants commonly used in Al Baha. Saudi Arabia, Adv Microbiol 8:938–949
Al-Hhedhairy AA, Wahab R (2022) Silver nanoparticles: an instantaneous solution for anticancer activity against human liver (HepG2) and breast (MCF-7) cancer cells. Metals 12(1):148
Ali A, Shah T, Ullah R et al (2021) Review on recent progress in magnetic nanoparticles: synthesis, characterization, and diverse applications. Front Chem 9:629054
Arif R, Uddin R (2021) A review on recent developments in the biosynthesis of silver nanoparticles and its biomedical applications. Med Devices Sens 4:e10158
Buttacavoli M, Albanese NN, Di CG et al (2018) Anticancer activity of biogenerated silver nanoparticles: an integrated proteomic investigation. Oncotarget 9(11):9685–9705
Chandralekha D, Shanmugam R, Madhuri K et al (2021) Review on silver nanoparticle synthesis method, antibacterial activity, drug delivery vehicles, and toxicity pathways: recent advances and future aspects. J Nanomaterials 2021:4401829
Chi CY, Wang F, Lei T, Xu SY, Hong AH, Cen YZ (2010) Studies on the chemical constituents from *Cissus pteroclada*. Zhong Yao Cai 33(10):1566–1568 (Chinese)
Cordani M, Somoza A (2019) Targeting autophagy using metallic nanoparticles: a promising strategy for cancer treatment. Cell Mol Life Sci 76(7):1215–1242
Datkhile KD, Patil SR, Durgawale PP et al (2020) Biogenic silver nanoparticles synthesized using mexican poppy plant inhibits cell growth in cancer cells through activation of intrinsic apoptosis pathway. Nano Biomed Eng 12(3):241–252
Datkhile KD, Durgawale PP, Patil MN et al (2021) Biosynthesis, characterization and evaluation of biological properties of biogenic gold nanoparticles synthesized using *Nothapodytes foetida* leaf extract. Nanosci Nanotec Asia 11(1):84–96
Dhanasekaran S (2020) Phytochemical characteristics of aerialpart of *Cissus quadrangularis* (L.) and its *in-vitro* inhibitory activity against leukemic cells and antioxidant properties. Saudi J Biol Sci 27(5):1302–1309
Elavazhagan T, Arunachalam KD (2011) Memecylon edule leaf extract mediated green synthesis of silver and gold nanoparticles. Int J Nanomed 6:1265–1278
Foldbjerg R, Dang AD, Autrup H (2011) Cytotoxicity and genotoxicity of silver nanoparticles in the human lung cancer cell line, A549. Arch Toxicol 85(7):743–750
Gardea-Torresdey JL, Gomez E, Peralta-Videa JR, Parsons JG, Troiani HE, Jose-Yacaman M (2003) Alfalfa sprouts: a natural source for the synthesis of silver nanoparticles. Langmuir 19(4):1357–1361
Ge C, Wang D, Ji D, Xu Z (2022) Green synthesized silver nanoparticle via *Cissus quadrangularis* as a theranostic agent for colon cancer. Int J Pharmacol 18(5):1047–1057
Gomes HIO, Martins CSM, Prior JAV (2021) Silver nanoparticles as carriers of anticancer drugs for efficient target treatment of cancer cells. Nanomaterials (basel) 11(4):964
Gummapu M, Amritkumar P (2019) Pharmacological properties of *Cissus quadrangularis* loaded silver nanoparticles: an in-vitro study. J Nanosci Curr Res 4(1):130

Gupta M, Arshad M, Shivnath N, Khan MS, Gupta R (2018) μCT analysis reveals that *Cissus quadrangularis* L. stem and *Trigonellafoenum-graecum* L. seed extracts prevent diabetic osteopathy. Indian J Tradit Knowl. 17(3):460–467
Gurunathan S, Han JW, Eppakayala V et al (2013) Cytotoxicity of biologically synthesized silver nanoparticles in MDA-MB-231 human breast cancer cells. Biomed Res Int 2013:535796
Haverkamp RG, Marshall AT (2009) The mechanism of metal nanoparticle formation in plants: limits on accumulation. J Nanopart Res 11(6):1453–1463
Huang J, Lin L, Sun D, Chen H, Yang D, Li Q (2015) Bio-inspired synthesis of metal nanomaterials and applications. Chem Soc Rev 44:6330–6374
Jadoun S, Chauhan NPS, Zarrintaj P, Barani M, Varma RS, Chinnam S, Rahdar A (2022) Synthesis of nanoparticles using microorganisms and their applications: a review. Environ Chem Lett 20(5):3153–3197
Jain N, Jain P, Rajput D, Patil UK (2021) Green synthesized plant-based silver nanoparticles: therapeutic prospective for anticancer and antiviral activity. Micro Nano Syst Lett 9(1):5
Kalpana VN, Patra RR, Rajeshwari VD (2017) Green synthesis of Zinc Oxide nanoparticles using fresh stem of *Cissus quadrangularis* extract and its various in vitro studies. Asian J Chem 29(6):1323–1327
Kanimozhi S, Durga R, Sabithasree M et al (2022) Biogenic synthesis of silver nanoparticle using *Cissus quadrangularis* extract and its in vitro study. J King Saud Univ- Sci 34(4):101930
Kasi SD, Ramasamy JM, Nagaraj D, Santiyagu V, Ponraj JS (2021) Biogenic synthesis of copper oxide nanoparticles using leaf extracts of *Cissus quadrangularis* and *Piper betle* and its antibacterial effects. Micro Nano Lett 16(8):419–424
Khan MA, Khan T, Nadhman A (2016) Applications of plant terpenoids in the synthesis of colloidal silver nanoparticles. Adv Colloid Interface Sci 234:132–141
Khandel P, Yadaw RK, Soni DK et al (2018) Biogenesis of metal nanoparticles and their pharmacological applications: present status and application prospects. J Nanostructure Chem 8:217–254
Kim W, Kwon HJ, Jung HY et al (2021) *Cissus verticillata* extract decreases neuronal damage induced by oxidative stress in HT22 cells and Ischemia in Gerbils by reducing the inflammation and phosphorylation of MAPKs. Plants 10(6):1217
Kolap RM, Gulave AB, Zimare SB (2020) Bioprospecting of the underutilized endemic taxon *Cissus woodrowii* (Stapf ex Cooke) Santapau for its antioxidant activity and phenolic profiling. Ind J Nat Product Resour 11(4):250–259
Kolap RM, Kakade PS, Mankar GD, Barmukh RB, Gacche RN, Zimare SB (2022) Bioprospection of underutilized wild *Cissus woodrowii* fruits for nutritional value and characterization of green-extracted antioxidant phenolic compounds. J Appl Res Med Aromat Plants 29:100379
Kumari R, Saini AK, Kumar A, Saini RV (2020) Apoptosis induction in lung and prostate cancer cells through silver nanoparticles synthesized from *Pinus roxburghii* bioactive fraction. J Biol Inorg Chem 25(1):23–37
Langer R, Weissleder R (2015) Nanotechnology: scientific discovery and the future of medicine. JAMA 313(2):135–136
Lu H, Zhang S, Wang J, Chen Q (2021) A Review on polymer and lipid-based nanocarriers and its application to nano-pharmaceutical and food-based systems. Front Nutr 8:783831
Marquis G, Ramasamy B, Banwarilal S, Munusamy AP (2016) Evaluation of antibacterial activity of plant mediated CaO nanoparticles using *Cissus quadrangularis* extract. J Photochem Photobiol B 155:28–33
Mejia-Mendez JL, Lopez-Mena ER, Sanchez-Arreola E (2023) Activities against lung cancer of biosynthesized silver nanoparticles: a review. Biomedicines 11(2):389
Menon S, Rajesh Kumar S, Venkat Kumar S (2017) A review on biogenic synthesis of gold nanoparticles, characterization, and its applications. Resource-Efficient Technol 3(4):516–527
Nagarajan K, Deyu L, Soundarpandian K (2019) Induction of intrinsic apoptotic signaling pathway in A549 lung cancer cells using silver nanoparticles from *Gossypium hirsutum* and evaluation of in vivo toxicity. Biotechnol Rep 23:e00339
Naidu KB, Govender P, Adam JK (2015) Biomedical applications and toxicity of nanosilver: a review. Med Technol SA 29(2):13–19
Patil PN, Singh SK, Wadkar KA (2023) Exploring the antioxidant potential of *Cissus woodrowii* (Stapf Ex Cooke) Santapau: a study on leaves and stem. Int J Drug Delivery Technol 13(4):1392–1398
Patil PN, Gilhotra RM, Sharma S, Wadkar KA (2024) Hepatoprotective and antioxidant activity of stem and leaves parts of *Cissus woodrowii* (Stapf ex Cooke) Santapau. Int J Pharm Quality Assur 15(2):588–594
Patra S, Mukherjee S, Barui AK, Ganguly A, Sreedhar B, Patra CR (2015) Green synthesis, characterization of gold and silver nanoparticles and their potential application for cancer therapeutics. Mater Sci Eng C 53:298–309
Patra JK, Das G, Fraceto LF et al (2018) Nano based drug delivery systems: recent developments and future prospects. J Nanobiotechnol 16(1):71
Rajeshkumar S, Menon S, Venkat Kumar S et al (2019) Antibacterial and antioxidant potential of biosynthesized copper nanoparticles mediated through *Cissus arnotiana* plant extract. J Photochem Photobiol B 197:111531
Rajeshkumar S, Menon S, Venkatkumar S et al (2021) Anti-inflammatory and antimicrobial potential of *Cissus quadrangularis*-assisted copper oxide nanoparticles. J Nanomater 2021:1
Ranoszek-Soliwoda K, Tomaszewska E, Malek K et al (2019) The synthesis of monodisperse silver nanoparticles with plant extracts. Colloids Surf B Biointerfaces 177:19–24
Renugadevi K, Inbakanandan D, Bhavanilatha M, Poornima V (2012) *Cissus quadrangularis* assisted biosynthesis of silver nanoparticles with antimicrobial and anticancer potentials. Int J Pharm BioSci 3(3):437–445
Sathappan S, Kirubakaran N, Gunasekaran D et al (2021) Green synthesis of zinc oxide nanoparticles (ZnO NPs) using *Cissus quadrangularis*: characterization, antimicrobial and anticancer studies. Proc Natl Acad Sci India Sect B Biol Sci 91(12):289–296
Sawangjit R, Puttarak P, Saokaew S, Chaiyakunapruk N (2017) Efficacy and safety of *Cissus quadrangularis* L. in clinical use: a systematic review and metaanalysis of randomized controlled trials. Phytother Res. 31(4):555–567
Siddiqui S, Zia Q, Abbas M, Verma S, Jafri A, Misra D, Luqman S, Ahamed M, Ahmad MS, Arshad M (2021) Antiproliferative activity of *Cissus quadrangularis* L. extract against human cervical cancer cells vitro and in silico analysis. Anticancer Agents Med Chem. 21(18):2536–2545
Singh P, Pandit S, Beshay M, Mokkapati VRSS, Garnaes J, Olsson ME, Sultan A, Mackevica A, Mateiu RV, Lutken H et al (2018) Anti-biofilm effects of gold and silver nanoparticles synthesized by the *Rhodiola rosea* rhizome extracts. Artif Cells Nanomed Biotechnol 8(46):886–899

Singh NB, Devi ML, Biona T, Sharma N, Das S, Chakravorty J, Rajashekar Y (2023) Phytochemical composition and antimicrobial activity of essential oil from the leaves of *Artemisia vulgaris* L. Molecules 28(5):2279
Sudharameshwari K, Maheshwari V (2017) *Cissus quadrangularis* extract mediated green synthesis of silver nanoparticles: pharmacological applications. Ind J Med Res Pharm Sci 4(8):30–36
Vijayaram S, Razafindralambo H, Sun YZ et al (2024) Applications of green synthesized metal nanoparticles—a review. Biol Trace Elem Res 202:360–386
Wu S, Rajeshkumar S, Madasamy M, Mahendran V (2020) Green synthesis of copper nanoparticles using *Cissus vitiginea* and its antioxidant and antibacterial activity against urinary tract infection pathogens. Artif Cells Nanomed Biotechnol 48(1):1153–1158
Yadi M, Mostafavi E, Saleh B, Davaran S, Aliyeva I, Khalilov R, Nikzamir M, Nikzamir N, Akbarzadeh A, Panahi Y et al (2018) Current developments in green synthesis of metallic nanoparticles using plant extracts: a review. Artif Cells Nanomed Biotechnol 46O:S336–S343
Yao Y, Zhou Y, Liu L et al (2020) Nanoparticle-based drug delivery in cancer therapy and its role in overcoming drug resistance. Front Mol Biosci 7:193
Yaqoob AA, Ahmad H, Parveen T et al (2020) Recent advances in metal decorated nanomaterials and their various biological applications: a Review. Front Chem 8:341

Publisher's Note